frontiers | Frontiers in Sustainability

TYPE Original Research
PUBLISHED 03 September 2025
DOI 10.3389/frsus.2025.1638375

OPEN ACCESS

EDITED BY
Huantian Cao,
University of Delaware, United States

REVIEWED BY
Piotr Smarzewski,
Military University of Technology in Warsaw, Poland
Ming-Qiang Zhu,
Northwest A and F University, China

*CORRESPONDENCE
Jose Suarez Loor
✉ jossloor@espol.edu.ec
Andrés Rigail Cedeño
✉ arigail@espol.edu.ec

RECEIVED 30 May 2025
ACCEPTED 17 August 2025
PUBLISHED 03 September 2025

CITATION
Loor JS, Cordero MC, Lazo M, Adrian E, López AM, Villalobos JV and Cedeño AR (2025) Sustainable thermoplastic elastomers: valorization of waste tires, recycled HDPE, and recycled EVA. *Front. Sustain.* 6:1638375. doi: 10.3389/frsus.2025.1638375

Sustainable thermoplastic elastomers: valorization of waste tires, recycled HDPE, and recycled EVA

Jose Suarez Loor[1]*, Miguel Carrasco Cordero[1], Miriam Lazo[1,2], Estephany Adrian[1,2], Angie Mendoza López[1,2], Joan Vera Villalobos[3] and Andrés Rigail Cedeño[1,2,4]*

[1]Facultad de Ingeniería en Mecánica y Ciencias de la Producción, ESPOL Polythecnic University, Guayaquil, Ecuador, [2]Laboratorio de Procesamiento de Plásticos, ESPOL Polythecnic University, Guayaquil, Ecuador, [3]Facultad de Ciencias Naturales y Matemáticas (FCNM), ESPOL Polytechnic University, Guayaquil, Ecuador, [4]Centro de Investigación y Desarrollo en Nanotecnología, ESPOL Polythecnic University, Guayaquil, Ecuador

The present study focused on the comprehensive investigation of the properties of thermoplastic elastomeric composites (TPE) containing 70% by weight of ground tire rubber (GTR) and a range of 15 to 30% by weight of recycled polyethylene (rHDPE). To improve the properties of these composites, different percentages of recycled nylon fibers (rPA) and recycled ethylene vinyl acetate (rEVA) were incorporated as reinforcing and compatibilizing agent, respectively. It was found that composites containing 5% and 10% by weight of rEVA exhibited higher plastic deformation capacity (7.3%), lower stiffness, and higher impact strength (247.92 J/m). These results were attributed to lower interfacial tension between GTR and rHDPE, which allowed the rHDPE to be encapsulated in the GTR matrix, thus favoring these mechanical properties. A detailed scanning electron microscopy (SEM) analysis revealed that the considerable particle size of the GTR used had a negative impact by causing premature tearing of the TPEs and limited deformability. Furthermore, it was confirmed that incorporating rPA into the composites adversely affected the mechanical, physical, and processability properties. This was due to difficulties in the homogeneous dispersion of rPA fibers within the GTR matrix. Also, when analyzing the processability of the composites, a slight increase in processing torque was observed in the composites with rEVA, which was attributed to a slight crosslinking of these composites. In contrast, thermogravimetric tests did not evidence a significant variation in degradation temperatures; however, they showed that the processing temperature should be kept below 380°C. These results highlight the considerable potential of the composites developed, as they have been manufactured exclusively from 100% recycled raw materials, without any physical or chemical pre-treatment.

KEYWORDS

ground tire rubber, tire waste fibers, thermoplastic elastomers, recycled high-density polyethylene, ethylene vinyl acetate

1 Introduction

In Ecuador, 8,800.000 units of End-of-Life Tires (ELTs) were managed for recycling between 2018 and 2025 (Seginus, n.d.). From a sustainability standpoint, this corresponds to a reduction of approximately 302,694 tons of carbon dioxide emissions into the environment (Seginus, n.d.). The primary entity responsible for this collective ELT management system is the SEGINUS corporation, established under the extended producer responsibility framework for national tire manufacturers (Seginus, n.d.). This comprehensive management system is especially critical when annual tire waste reaches nearly 4 million units (El Universo, 2024). The inadequate treatment of such waste results in the emission of toxic organic and inorganic pollutants into the atmosphere (Acevedo et al., 2015), soil (Wade and Simek, 2012), and water (Tham et al., 2016), as well as contamination of surrounding habitats. Consequently, local commercial initiatives have been developed to repurpose tire waste into flooring and shoe soles (63%), handicrafts (2%), pyrolysis-derived products (18%), cogeneration fuel (14%), and synthetic sports fields (5%) (Seginus, n.d.). Despite its potential, the combination of tire waste and widely used plastics like polyolefins to upcycle ground tire rubber (GTR) remains unexplored. In 2022 alone, thermoplastic waste in Ecuador amounted to 627,000 tons (Ministerio del Ambiente A y TE, n.d.). Like ELTs, poor management of these materials poses serious environmental risks. Therefore, there is a clear opportunity to develop alternative waste stream materials and define their potential applications as substitutes for conventional practices.

Transforming waste into functional materials poses several technical challenges, especially when dealing with ELTs due to their complex composition. These materials consist of a mixture of elastomers, carbon black or silica, steel wires, textile fibers (Yilmaz, 2007), vulcanizing agents, additives (Zhang et al., 2007), and sulfur. In response, various valorization strategies have been developed, including pyrolysis, retreading, incineration, and blending with other materials (Fazli and Rodrigue, 2022a). The latter approach, involving the grinding of tires into granulated rubber (GTR), enables the formulation of new materials, especially thermoplastic elastomers (TPEs), by mixing GTR with thermoplastic matrices. These compounds have demonstrated recyclability, cost-efficiency, low density, and satisfactory mechanical performance (Fazli and Rodrigue, 2022a), provided that adequate compatibility and dispersion are achieved by controlling variables such as particle size, GTR concentration, the nature of the base material, and the interactions between the components (Periasamy et al., 2023).

When a higher concentration of GTR is used in the composite, low strains are achieved (Liu et al., 2022). A TPE for low strain is generally considered suitable for flexible sensors, damping pads, elastomeric keypads, or static seals (Biemond and Gaymans, 2010; Persson and Andreassen, 2022). Furthermore, synthesizing TPEs is challenging due to the poor compatibility between GTR and thermoplastic matrices, which arises from rubber's crosslinked nature (Fazli and Rodrigue, 2022a). To address this issue, two primary approaches have been proposed: rubber devulcanization and surface modification of GTR particles. However, both methods have their drawbacks. Devulcanization can compromise the integrity of the rubber and lead to degradation (Kiss et al., 2022), while physical modifications require high energy inputs (Periasamy et al., 2023), and chemical treatments often involve hazardous reagents (Badiee, 2016). As an alternative, non-reactive compatibilization strategies have emerged, including using copolymers with affinity for both phases. Additives such as EVA (Ramarad et al., 2015), SBS (de Oliveira et al., 2018), EOC (de Oliveira et al., 2018), TOR, EPDM, and maleic anhydride-grafted polyolefins have been shown to enhance interfacial adhesion, which is critical to achieving desirable functional properties (Li et al., 2021). The choice of the base thermoplastic is crucial. Among the most common plastic wastes are PET, HDPE, PP, and LDPE (Ahmadian et al., 2020). Recycled HDPE (rHDPE) is particularly promising for blending with GTR due to its lower processing temperature, greater availability, and reduced moisture sensitivity.

One often-overlooked ELT component is the textile fraction, composed of fibers such as nylon, polyester, rayon, or aramid (Wang et al., 2021). After tire shredding, these fibers are typically contaminated with rubber particles, limiting their reuse and often relegating them to landfills or incineration. Nevertheless, their incorporation as reinforcement within TPE composites represents a promising alternative for valorization, and their effect on mechanical properties will be evaluated. On the other hand, according to Zhang et al. (2007), incorporating EVA as a compatibilizer in HDPE/GTR has improved impact strength and an increase of elongation at break by 175 J/m and 82%, respectively. Fazli showed that using recycled EVA might form an encapsulating interface that increases the deformability and toughness of the material (Patrício et al., 2021). However, fibers and recycled EVA have not yet been included in a GTR/rHDPE. Therefore, this work aims to prepare a TPE employing rHDPE and 70 wt.% GTR, with recycled ethylene-vinyl acetate (rEVA) and tire textile fibers (rPA) as compatibilizer and filler, respectively. This type of TPE would be intended for applications such as roof or floor tires, where high structural strength and elongation are not required. Therefore, the material can have a high filler content and be highly recyclable.

2 Materials and methods

2.1 Materials

GTR with a particle size greater than 1 mm and rPA were used as the matrix and filler, respectively. These raw materials were supplied by the Ecuadorian Integrated Used Tire Management System Corporation SEGINUS S.A. (Guayaquil, Ecuador). rEVA from sandals was donated by PICA Plásticos Industriales C.A. (Guayaquil, Ecuador) and used as a compatibilizer. Finally, injection grade rHDPE with a Melt Flow Rate of 7 g/10 min was provided by NOVARED-NEGOCIOS Y RECICLAJE S.A. (Guayaquil, Ecuador).

2.2 Sample preparation

In this study, the effects of adding rEVA and rPA on a GTR/rHDPE matrix will be evaluated, and it will be represented as M. Herein, GTR was kept constant at 70 wt.% to prioritize the utilization of this waste. At the same time, the weight percentage of rHDPE varied according to the proportion of the rest of the components. Three percentages of rEVA were considered: 0, 5, and 10 wt.%, and two for rPA: 0 and 5 wt.%. Table 1 shows the nomenclature used for the samples.

TABLE 1 Proportions of components.

Sample	GTR (wt.%)	rHDPE (wt.%)	rEVA (wt.%)	rPA (%)
M-0rEVA-0rPA	70	30	0	0
M-5rEVA-0rPA		25	5	0
M-10rEVA-0rPA		20	10	0
M-0rEVA-5rPA		25	0	5
M-5rEVA-5rPA		20	5	5
M-10rEVA-5rPA		15	10	5

GTR, rEVA, and rHDPE were used as received. On the contrary, rPA was dried at 80 °C for 24 h in a muffle oven (QUIMIS®, Brazil). All components were melted and blended at 200 °C and 70 rpm for 10 min in a Brabender Plastograph® EC Plus torque rheometer. The temperature was set to avoid further decomposition of GTR (Acevedo et al., 2015). Additionally, the rPA in use exhibits thermal instability beyond 200 °C. Next, 200 mm × 200 mm × 3 mm sheets were prepared using a hydraulic press at 2,000 psi and 200 °C for 10 min. Finally, specimens for mechanical testing were die-cut.

2.3 Processability

The processability of the composite was evaluated using a Brabender Plastograph® EC Plus torque rheometer. Samples (35 g) were processed at 200 °C and 90 rpm for 10 min. The rheometer provided data on flow behavior, and specific energy consumption required (SEC) to process the TPE formulations. Equation 1 shows the specific energy consumption (SEC), where the $\int Mdt$ refers to the integral under the curve for the torque-time plot in N·m·min, N is the speed in min^{-1}, and m is the mass processed in kg (Carrasco et al., 2023).

$$SEC = \frac{N\int_0^{t_\infty} Mdt}{m}\left[kW.h/kg\right] \quad (1)$$

2.4 Characterization

2.4.1 Fourier transform infrared spectroscopy (FTIR)

Fourier transform infrared (FTIR) spectroscopy was conducted using a Thermo Scientific iS10 model equipped with a Horizontal Attenuated Total Reflectance (HATR) accessory and a multi-bounce ZnSe crystal, set at a 45-degree angle. The spectra were recorded in the mid-infrared range, from 4,500 to 450 cm^{-1}, to analyze the raw materials and assess potential reactions between their functional groups. The sample geometry consisted of circular films with a diameter of 3 mm and a thickness of 1 mm.

2.4.2 Scanning electron microscopy (SEM)

The average particle size of the GTR used in the TPEs was identified, and micrographs of the fractured surfaces of the blends were used to observe phase distribution and compatibility. A FEI Inspect S50 scanning electron microscope (Hillsboro, OR, USA) was used. The equipment was operated in high vacuum mode with a voltage of 15 kV, a 3-point, and a backscatter detector.

2.4.3 Contact angle measurement

The sessile drop method was employed to evaluate the compatibilizing effect of rEVA by measuring the contact angle of GTR, rHDPE, and rEVA at room temperature. The liquids considered were water, dimethyl sulfoxide (DMSO) and glycerol. The angles were estimated using ImageJ software and the average angles of five replicates are reported. Herein, the interfacial energy of pairs (GTR/rHDPE, rHDPE/EVA and GTR/rHDPE) were estimated using Wu's harmonic mean model shown in Equation 2:

$$\gamma_{ij} = \gamma_i + \gamma_j - \frac{4\gamma_i^p\gamma_j^p}{\gamma_i^p + \gamma_j^p} - \frac{4\gamma_i^d\gamma_j^d}{\gamma_i^d + \gamma_j^d} \quad (2)$$

γ_{ij} is the interfacial energy between materials i and j; γ_i is the surface energy of the i, γ_i^d is the dispersive contribution of i and, γ_i^p its polar component. On the other hand, the spreading coefficient (λ_{ijk}) helps determine the most probable arrangement of the analyzed ternary system, and it can be obtained from the calculated surface energies through Equation 3:

$$\lambda_{ijk} = \gamma_{ik} - \left(\gamma_{ij} + \gamma_{jk}\right) \quad (3)$$

2.4.4 Thermogravimetric analysis (TGA)

Thermal stability and degradation temperature were investigated using a TA Instruments Q600 STD (TGA/DSC) analyzer. The test was carried out at a heating rate of 10 °C·min^{-1} in a nitrogen atmosphere (100 mL·min^{-1}) from room temperature up to 700 °C.

2.5 Mechanical testing

Tensile properties were assessed using ASTM D638 at a 5 mm/min rate in a Shimadzu AG-IS (10 kN) universal testing frame. A three-point bending test was performed based on ASTM D790 at a rate of 50 mm/min at room temperature and using the previous equipment. An impact resistance test with a Jin Jian pendulum was conducted on unnotched specimens following ASTM D256.

The Shore A hardness test followed ASTM D2240, which applies to hard or soft rubbers and thermoplastic elastomers. The equipment used was a Qualitest HPE-II and 15 measurements were considered. Finally, the compression set test using Method B (constant deflection) from ASTM D395 was conducted to evaluate the retention of elastic properties after prolonged exposure to compressive stress.

2.6 Techno-economic analysis

This techno-economic study was feasible for tile production based on the material with the highest score in the decision matrix. The study included an estimation of the total capital investment and an analysis of project profitability through indicators such as the Internal Rate of Return (IRR), Net Present Value (NPV), and Return on Investment Period (RIP), following the methodology proposed by Barcia-Quimi et al. (2023). The analysis considered a project lifetime of 10 years plus 1 year for plant construction. An interest rate of 8.52%

and a tax rate of 15% were applied. Maintenance and administrative costs were estimated at 18% of the capital investment.

2.7 Carbon footprint and energy demand calculations

An eco-audit was conducted to evaluate the carbon footprint and energy demand of the final product, using the methodology proposed by Ashby (2012). This method enables a rapid assessment of the energy requirements and carbon emissions associated with the product's life cycle. The analysis covered the stages of material extraction, manufacturing, transportation, use, and end-of-life disposal, as presented in Table 2.

3 Results and discussion

3.1 Torque rheometer analysis: processability and specific consumed energy

In Figure 1a, the behavior and interactions of polymers, fillers, and additives during the processing stage are examined (Rigail-Cedeño et al., 2022), which is indirectly proportional to the processing torque in the case of conventional manufacturing processes such as extrusion. In this case, torque is associated with a measure proportional to viscosity. Figure 1a shows an increase in melting and stabilized torque as the percentage of rEVA and rPA in the composites increases. The increase in torque related to the presence of rEVA is associated, according to Goharpey et al. (2005) and Farias et al. (2021), with the decrease in free volumes and limited rotational mobility of the rHDPE in the mixing chamber. This effect may be due to two reasons. The first is due to contaminants and some degree of degradation in the recycled EVA. On the other hand, the second is associated with some compatibilization and minimal *in situ* vulcanization of the rEVA-containing TPE in the mixing chamber

TABLE 2 Eco-audit equations.

Stage description	Mathematical expression
Energy and carbon footprint by disposal	$E_{disposal} = E_{Re} + E_C \left[MJ/kg \right]$ (4)
	$CO2_{disposal} = 0.07 \times E_{disposal} \left[Kg\, CO_2 \right]$ (5)
Energy and carbon footprint at the end of life (End of Life, EoL)	$H_r = r\left(\tilde{H} - H_{RC}\right)\left[MJ/kg \right]$ (6)
	$CO2r = r\left(\tilde{C} - C_{RC}\right)\left[kg/kg \right]$ (7)
Energy and carbon footprint effective	$\tilde{H} = RH_{RC} + (1-R)H_m \left[MJ/kg \right]$ (8)
	$\tilde{C} = RH_{RC} + (1-R)C_m \left[kg/kg \right]$ (9)

E_{Re} y E_C represent the equivalent energy for the collection and classification of materials, respectively. r denotes the content of recyclable material at the end of the life cycle. H_{RC} y C_{RC} refer to the energy and environmental footprint associated with the recycling process, respectively. H_m y C_m correspond to the energy and environmental footprint incorporated related to virgin material production. R indicates the initial content of recycled material at the beginning of the life cycle.

(Farias et al., 2021). This may be a product of the interaction of GTR and rEVA due to their elastomeric character (Mészáros et al., 2008). This behavior is observed in Figure 1a, which exhibits a trend of increasing processing torque shortly after the initial melting torque (at approximately 1.5 min) in the samples with rEVA. Finally, incorporating rPA into the TPEs showed a more significant increase in torque than rEVA alone. This is due to increased collisions between melt particles and filler (Abraham and George, 2009). This increases the probability of fiber agglomerations, which are observed in SEM micrographs and result in lower mechanical properties.

In Figure 1b, it was established that optimal processability is associated with minimizing energy consumption. The material with the lowest energy consumption was M-0rEVA-0rPA, while the material with the highest consumption was M-10rEVA-5rPA. This contrast indicates that adding fibers and a compatibilizer increases the energy required for material homogenization. This is attributed to fiber agglomeration, the reduction of free volume, and the restriction of molecular mobility caused by the incorporation of rEVA (Alothman, 2012). This behavior was also observed in the torque versus time curves used to calculate energy consumption (Figure 1a), where the lowest torque values corresponded to the sample without aggregate.

3.2 Characterization

3.2.1 Fourier transform infrared spectroscopy (FTIR)

The FTIR spectrum of the GTR (Figure 2a) shows peaks at the 3,424, 2,900, 1,600, 1,400, and 1,000 cm^{-1}. The low peak at 3,424 cm^{-1}, according to Naat et al. (2021) and Panwar et al. (2015), is due to the symmetric stretching of the OH group that is present in the silica used as filler in tires, as well as the stretching of the system Si–O–Si that presents a peak at about 1,025 cm^{-1}. The 2,900 cm^{-1} peak corresponds to the stretching of the C–H group present in SBR and NBR polymers. The band of peaks at 1,600 and 1,400 cm^{-1} are related to the C=H vibrations and bending vibrations of the C–H bonds present in the phenyl group of SBR (Kazemi et al., 2023). Finally, the band at 1,000 cm^{-1} shows symmetrical stretching vibrations of the C–O and C–N bonds, which, according to Fazli and Rodrigue (2020a), are related to the presence of additives and nitrile groups of NBR, respectively.

Figure 2b shows the FTIR spectrum of rPA with characteristic peaks in the 3,400, 2,911, and 1,640 cm^{-1} bands. The 3,400 cm^{-1} peak represents the symmetric stretching of the N–H bond belonging to the structure of a secondary amide; this is because a second asymmetric stretching is not observed (Wade and Simek, 2012). The 2,911 cm^{-1} peak corresponds to the stretching of the unsaturated C–H bonds, which are part of the main structure of a polyamide (Kazemi et al., 2023). At last, the carbonyl group (C=O) of the rPAs is represented at IR frequencies near 1,640 and 1,680 cm^{-1} (Wade and Simek, 2012). These results indicate that rPA obtained from waste tires can be nylon 6,6 or a mixture of both in the form of fibers (Acevedo et al., 2015).

The rEVA and rHDPE spectra (Figures 2c,d) show the same peak at the 2,900 cm^{-1} wavelength due to the vibration of the C–H bond present in the ethylene repeating unit and a peak between the 1,400 and 1,439 band due to the scissor vibration of the CH_2 groups (Wade

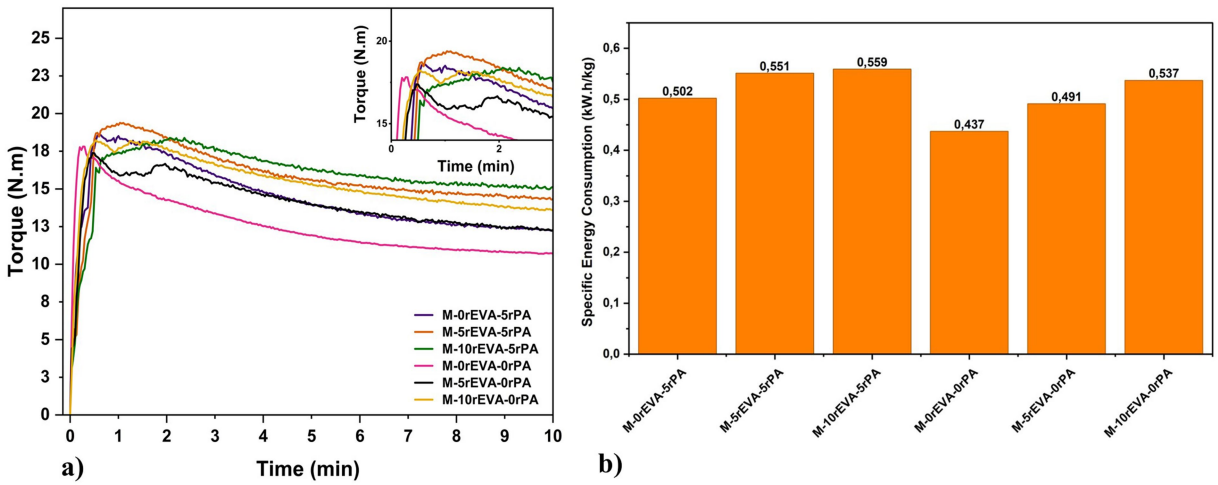

FIGURE 1
(a) Processability of TPE: Torque-time curves, **(b)** specific energy consumption.

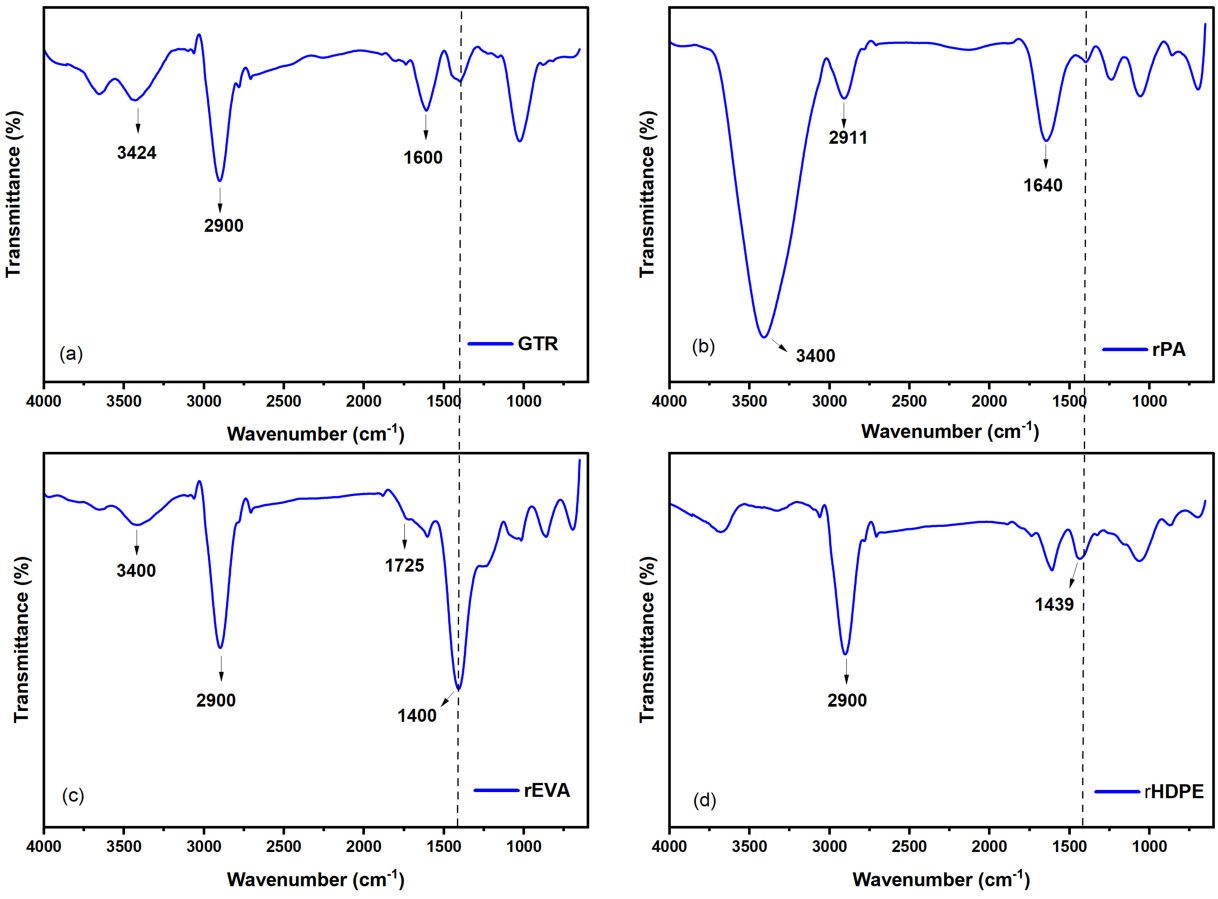

FIGURE 2
FTIR spectra of raw materials with digital print at 1400 cm^{-1}. **(a)** GTR, **(b)** rPA, **(c)** rEVA and **(d)** rHDPE.

and Simek, 2012). The rEVA spectrum shows a peak around 1,725 cm^{-1}, corresponding to the carbonyl group stretching in the copolymer's acetate repeating unit (Tham et al., 2016). The absorption of this C=O group, according to Wade and Simek (2012), produces a harmonic band around 3,400 cm^{-1}, which is assigned to O–H stretching of hydroxyl groups (Allen et al., n.d.). The reprocessing of recycled EVA can explain the minor band of the carbonyl group, as constant exposure to high temperatures causes EVA degradation and

the loss of acetate units, followed by the concurrent formation of hydroxyl species on the material's surface (Allen et al., n.d.).

Figure 3 presents the FTIR spectra of the compound blends with varying contents of rEVA and rPA. All samples show prominent peaks around 2,900 cm^{-1}, 1,600 cm^{-1}, and 1,400 cm^{-1}. The absorption at ~2,900 cm^{-1} is attributed to C–H stretching vibrations, characteristic of both the rubber matrix (SBR/NBR) and ethylene units (Wade and Simek, 2012; Kazemi et al., 2023). Peaks near 1,600 cm^{-1} and 1,400 cm^{-1} correspond to C=C and C–H bending vibrations from the phenyl groups of SBR (Kazemi et al., 2023).

Blends containing rPA fibers—namely spectra (g), (h), and (j)—exhibit an additional broad peak at approximately 3,400 cm^{-1}, corresponding to N–H stretching vibrations in secondary amides (Wade and Simek, 2012). This feature is absent in the blends without rPA (e, f, i), confirming the contribution of polyamide-based fiber residues.

Among the samples containing rEVA—specifically (g), (i), and (j)—a notable increase in the intensity of the 1,400 cm^{-1} peak is observed, attributed to the scissoring vibration of CH_2 groups in the EVA chains (Wade and Simek, 2012). This peak is less intense or absent in the spectra without rEVA (e, f, h), further confirming the

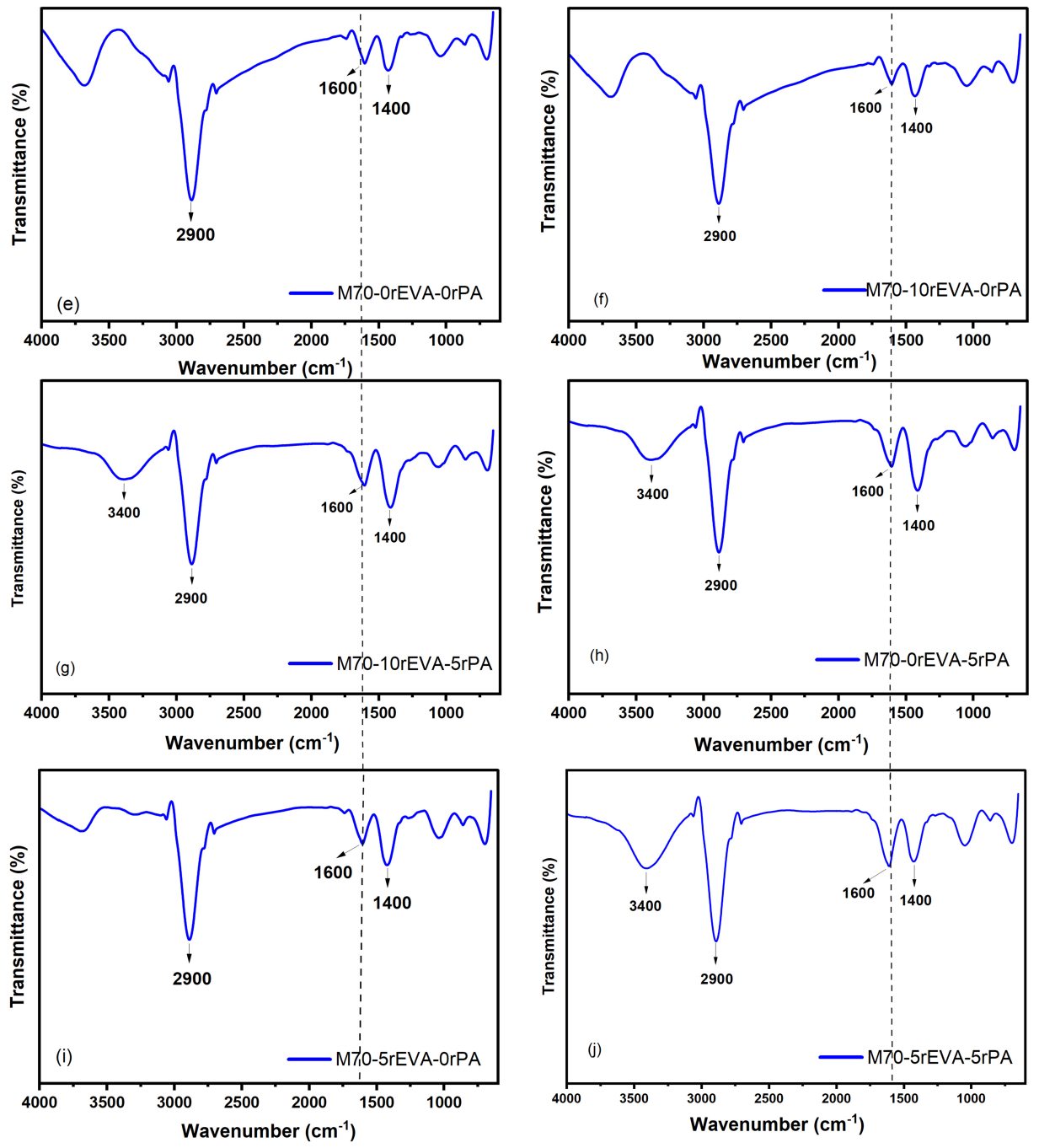

FIGURE 3
FTIR spectra of composites with digital print at 1600 cm^{-1}. **(e)** M70-0rEVA-0rPA, **(f)** M70-10rEVA-0rPA, **(g)** M70-10rEVA-5rPA, **(h)** M70-0rEVA-5rPA, **(i)** M70-5rEVA-0rPA and **(j)** M70-5rEVA-5rPA.

contribution of the copolymer. In addition, in these rEVA-rich samples, the shoulder around 2,900 cm^{-1} appears slightly broadened, which may indicate overlapping contributions from rubber and EVA components. Furthermore, the peak around 1,600 cm^{-1} shows higher intensity in samples containing rPA due to the contribution of C=O stretching in amide groups. This overlap may mask or enhance signals from the rubber matrix, indicating complex interactions.

3.2.2 Scanning electron microscopy (SEM)

The morphology of the compounds listed in Table 1 was analyzed at magnifications from 500 to 2,000×. In general, in all the micrographs in Figure 4, a non-homogeneous microstructure can be seen due to the high concentration of rubber (70 wt.%) and the low dispersion of the semi-crystalline thermoplastic in the highly crosslinked GTR matrix (Fazli and Rodrigue, 2022a).

The micrographs in Figures 4a,b correspond to M-0rEVA-0rPA. In the first one, a smooth fracture surface of the GTR surrounded by the rHDPE was observed, with a space between them. According to Fazli and Rodrigue (2022a), this type of fracture is characteristic of low interfacial adhesion and high incompatibility between the GTR particles, and the thermoplastic used, implying a limited plastic deformation capacity before fracture (Fazli and Rodrigue, 2022a). The gaps between the GTR/rHDPE interface are attributed to a high surface energy of the composite, resulting in an inefficient stress transfer mechanism. This behaves as predicted by the studies of Li et al. (2004), which calculated that all binary GTR/HDPE blends had higher interfacial stresses than their ternary counterparts with added elastomers.

Micrograph (b) exhibits voids throughout the composite, associated with the rubber's high crosslinking and elastomeric nature, preventing chemical interaction and only promoting physical interaction with the rHDPE. This weak adhesion between these materials reduces the load transfer capacity between phases, initiating a premature failure in the composite, which is reaffirmed in the results of the tension and flexural tests (Periasamy et al., 2023).

In contrast, the micrograph of the M-10rEVA-0rPA material (Figure 4c) presented a better interaction between the GTR/rEVA/rHDPE phases. In this one, a rough fracture surface can be observed, implying a higher plastic deformation capacity (evidenced by the traction and bending results) thanks to the compatibilizing effect of rEVA as a coupling agent due to its elastomeric character that allows the encapsulation of the dispersed phase during the mixing process under the melting (Kiss et al., 2022; Mészáros et al., 2008). However, voids around rubber particles were still evident, which can be justified by possible contaminants and impurities in the rEVA (Badiee, 2016; de Oliveira et al., 2018) and the high particle size of the GTR (Ramarad et al., 2015).

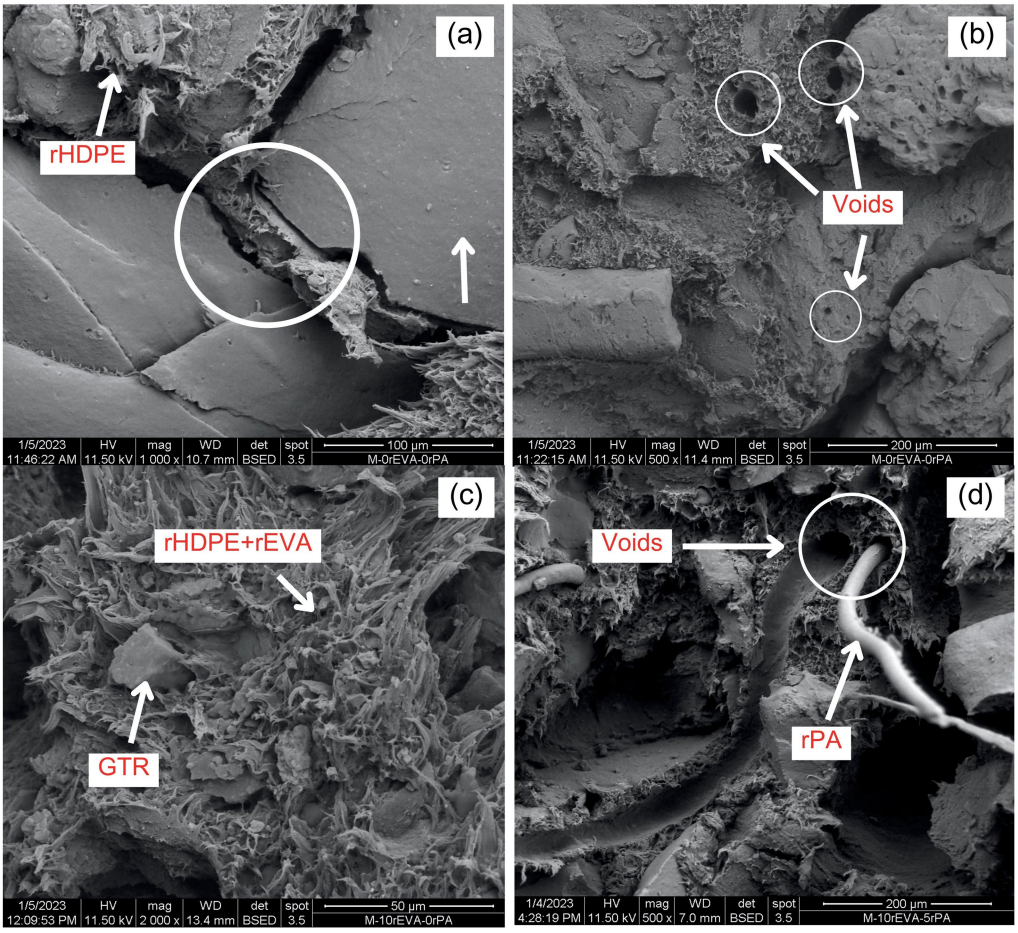

FIGURE 4
SEM micrograph of **(a)** and **(b)** M-0rEVA-0rPA, **(c)** M-10rEVA-0rPA and **(d)** M-10rEVA-5rPA.

Although GTR particles larger than 1 mm were observed to induce microstructural voids and poor compatibility within the matrix, reducing their size involves significant economic and energy considerations. Grinding GTR to particles smaller than 250 μm (Kiss et al., 2022)—the ideal size for enhancing interaction with thermoplastic matrices—requires multiple stages of comminution, which substantially increases energy consumption and equipment wear. Furthermore, as particle size decreases, the tendency of GTR to agglomerate rises due to its high surface-to-volume ratio, potentially hindering processability and increasing the viscosity of the compound during mixing (Zhang et al., 2007). Therefore, while a finer granulometry may improve compatibility and the mechanical performance of the composite, this benefit must be weighed against the higher energy demands and additional dispersion challenges encountered during processing.

Finally, an evident heterogeneity (voids and fiber agglomeration) could be observed in the micrograph of the M-10rEVA-5rPA formulation (Figure 4d). According to Mészáros et al. (2008), this morphology is the product of the low chemical interaction of the polar polyamides with the nonpolar GTR/rHDPE interface, creating fiber-rich and resin-rich zones (Li et al., 2021). According to Ahmadian et al. (2020), this factor decreases mechanical properties such as stiffness and fracture toughness (Barbero, 2016).

3.2.3 Contact angle measurement

The interfacial tension between the GTR/rEVA/rHDPE components and the spreading coefficients were obtained to know the morphology of the phases (Palakattukunnel et al., 2011). Based on Table 3, the GTR/rHDPE pair is highly immiscible, considering their high interfacial tension (5.98 mN/m) and negative coefficient value (−3.69), so these materials tend to separate. The lower energy of rHDPE/rEVA, concerning GTR/rEVA and GTR/rHDPE, and a positive dispersion coefficient (2.43) suggest that the system is thermodynamically more stable when rEVA encapsulates rHDPE in the rubber matrix due to higher partial wetting (Fazli and Rodrigue, 2021). This morphology is directly related to the results obtained in the FTIR test. Intermolecular London dispersion interactions between the ethylene segments of rHDPE and rEVA and Van de Waals forces between the acetate group of rEVA could explain it (Yilmaz, 2007) and oxygen-containing functional groups in the GTR (Figures 5a,b), as well as the possible presence of residual oxygen molecules on its surface (Zhang et al., 2007).

TABLE 3 Interfacial tension of the ternary system GTR/rHDPE/rEVA and spreading coefficient.

Polymer pairs	Interfacial tension (mN/m)	Spreading coefficient
GTR/rHDPE	5.98	−3.69
GTR/rEVA	2.92	−8.26
rHDPE/rEVA	0.63	2.43

3.2.4 Thermogravimetric analysis (TGA)

Figures 6a,b show the thermogravimetric curves (TGA) and their derivative (DTG) of the raw materials used. Initially, it was observed that the maximum degradation of rHDPE and rEVA occurs at 490 and 474 °C, respectively. This behavior is due to the decomposition and volatilization of the hydrocarbon chain of which they are composed. Unlike rHDPE, rEVA exhibited a 48% residual mass, which is attributed to calcium carbonate as a residue. The GTR curves show a double-peak behavior. Regarding this, the first peak (310 °C) denotes the volatilization of commercial oils and additives used for tire manufacturing. On the other hand, the second peak (415 °C) corresponds to the thermal degradation of the polymers in the GTR structure (Fazli and Rodrigue, 2022a). GTR exhibited a 37% residual mass, attributed to the presence of carbon black in its structure. On the other hand, it is observed that rPA decomposition occurs around 367 °C and achieves its maximum thermal degradation at 413 °C, which is a typical behavior of Nylon 6 fibers (Kamran et al., 2022). In this case, rPA exhibited a 23% residual mass, due to contamination with GTR.

Regarding the synthesized TPE materials (Figures 6c,d), initially, the outgassing of volatiles from processing oils or additives was observed

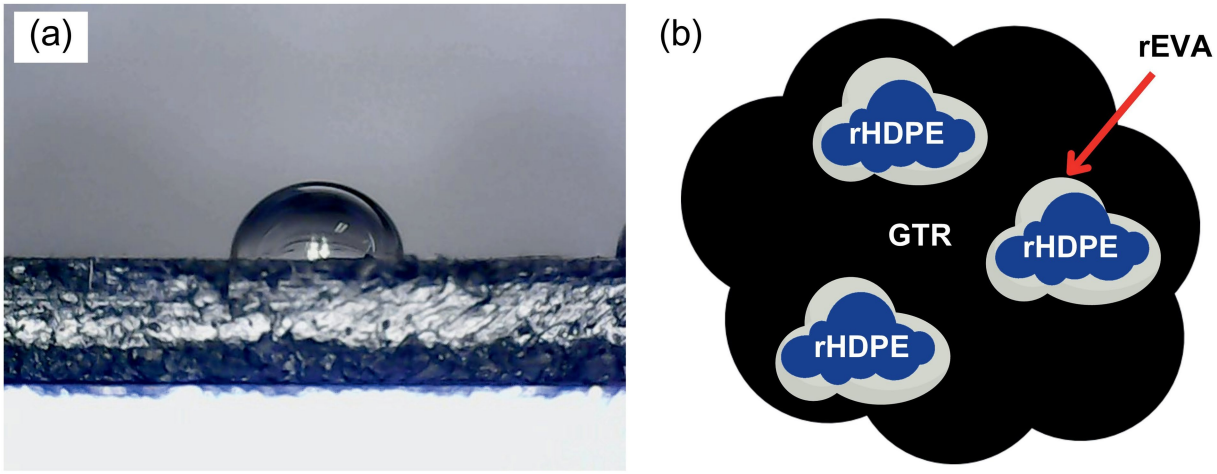

FIGURE 5
(a) Contact angle measurement of GTR composites and **(b)** proposed chemical interaction model of TPEs.

as a reduction of 18–20 wt.% near 50 °C. This was followed by a 43.4% mass loss associated with the thermal degradation of thermoplastics and elastomers (natural and synthetic, recycled) (Wang et al., 2021; van Hoek et al., 2019) between 380 and 480 °C. This double peak (Figure 6d) may be due to the decomposition of rEVA in the composite matrix. The first peak (380 °C) is related to a deacetylation reaction, in which, according to Fazli and Rodrigue (2022a), acetic acid is released, and the formation of ethylene bonds along the polymer backbone begins. Finally, the second peak corresponds to the degradation of the remaining hydrocarbon (ethylene group).

The remaining components (38%) (Figure 6c) were carbon black and inorganic fillers such as silica. Finally, Figure 6d represents the derivative of the weight change concerning temperature. No significant variation in peak position was found due to rEVA and rPA. These thermogravimetric results infer that the composites should not be processed above 380 °C and that the TPEs can be reprocessed under the same synthesis conditions proposed in the present investigation.

3.3 Mechanical testing

Mechanical testing was conducted to assess the suitability of the developed TPEs for applications requiring flexibility, impact resistance, and durability. The selection of mechanical properties was based on the target application and the role of each recycled component within the composite system.

3.3.1 Tensile test

Figure 7a shows the tensile strength of blends with and without rPA as a reinforcing agent as a function of the percentage of rEVA. A notable reduction in tensile strength is observed as the percentage of rEVA increases. Concerning TPE without fibers, a significant decrease in tensile strength was observed when adding 5 and 10 wt.% rEVA, going from 2.92 to 2.67 MPa (−8.92%) to 2.49 MPa (−14.02%), respectively. Likewise, a similar response in reducing this property was observed for the rPA-containing TPEs, with a decrease of 10.91% (2.45–2.1 MPa) with 5 wt.% rEVA and 14.02% (2.45–2.11 MPa) with 10 wt.% rEVA.

Since GTR is a crosslinked material with an elastomeric nature, rEVA acted as a compatibilizing agent in TPEs with and without fiber, improving the interaction between the matrix phase and rHDPE (Fazli and Rodrigue, 2022a), decreasing the tensile strength due to its soft and rubbery character (Mészáros et al., 2008). On the other hand, it was observed that TPEs with rPA had lower performance, which may be due to a combined effect of two factors. The first is the significant reduction in the amount of

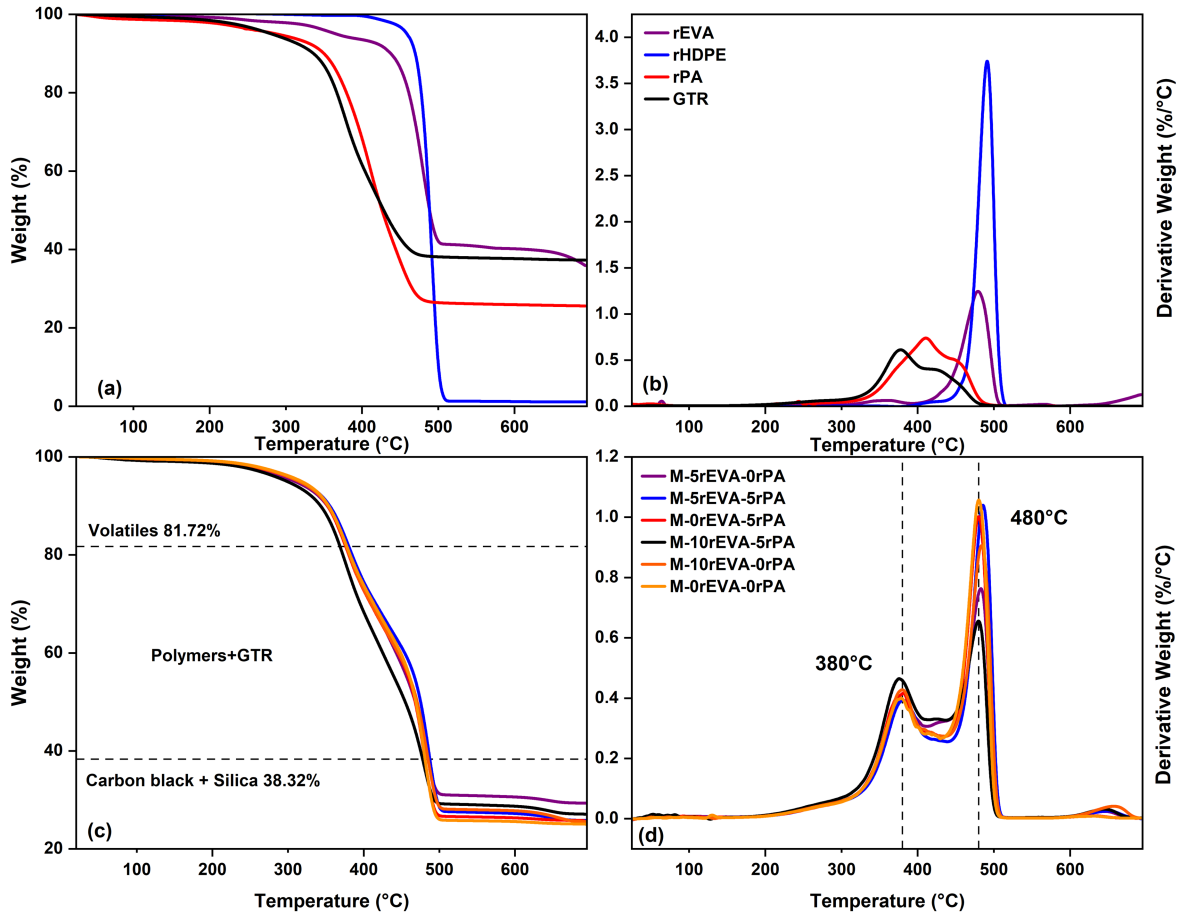

FIGURE 6
TGA analysis for raw materials: **(a)** Weight variation versus temperature, and **(b)** Degradation temperature ranges. TGA analysis for TPEs: **(c)** Weight variation versus temperature, and **(d)** Degradation temperature ranges.

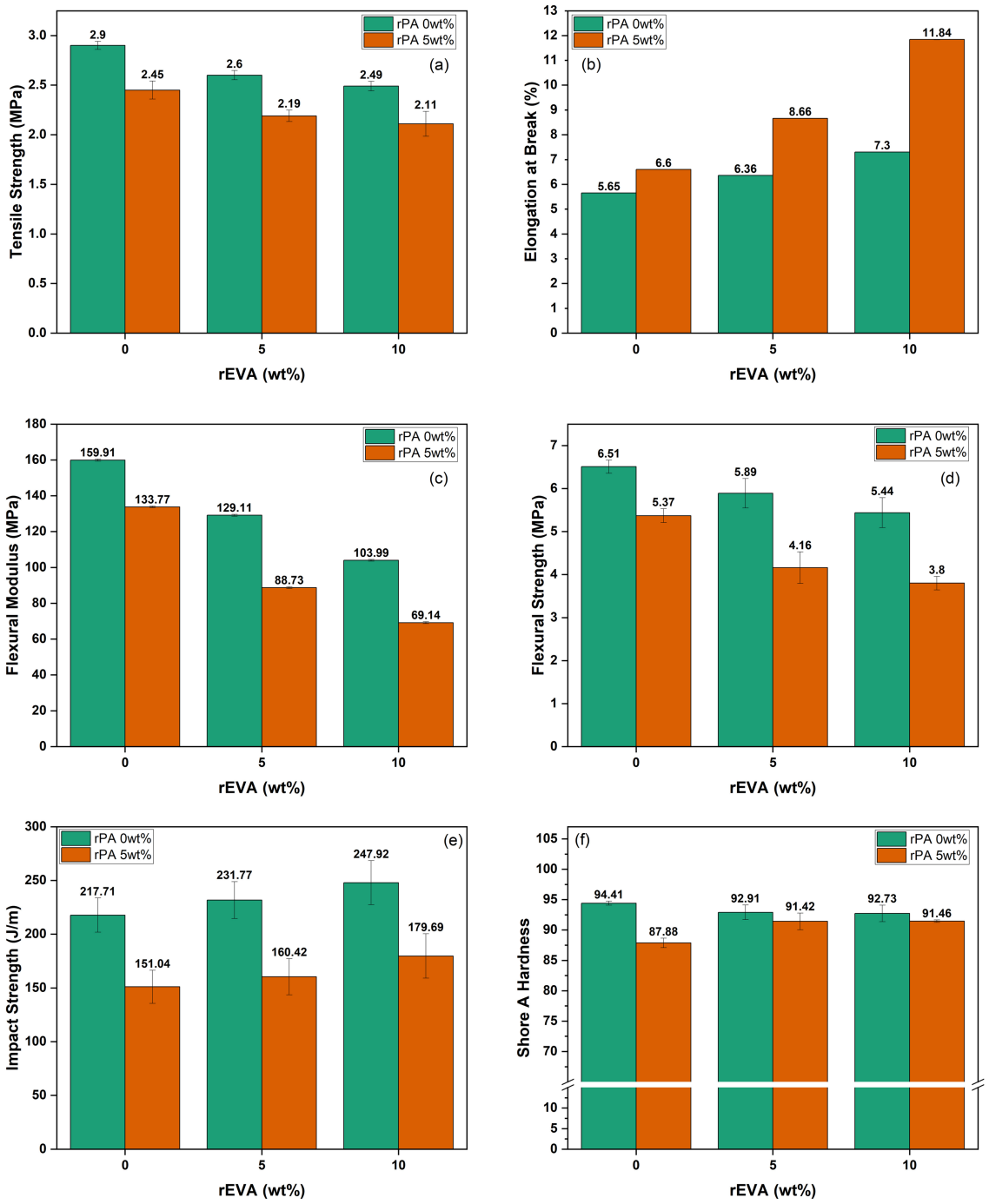

FIGURE 7
TPEs mechanical properties: **(a)** tensile strength, **(b)** elongation at break, **(c)** flexural modulus, **(d)** flexural strength, **(e)** IZOD impact strength, and **(f)** Shore A hardness.

rHDPE of up to 15 wt.%, which is a semi-crystalline polymer, significantly contributing to tensile strength. Secondly, the polar and hydrophilic character of rPA, mainly polyamides (Patrício et al., 2021), causes possible resin-rich zones and zones with fiber agglomeration due to the repulsion of these with the non-polar segments of the GTR/rHDPE, resulting in stress concentration zones in the material and sudden cracking at the GTR/rHDPE interface (Sebaey et al., 2021).

As stated in Fazli and Rodrigue (2022a), elongation at fracture is a fundamental mechanical parameter for classifying functional TPEs, as it directly reflects the interfacial compatibility and homogeneity of the polymer system. In this work, all the composites developed presented values at a maximum of 11.84% (Figure 7b), evidencing possible structural limitations of using recycled materials. This behavior is mainly attributed to (1) the cross-linked nature of the GTR, which prevents adequate adhesion with the

rHDPE matrix due to the absence of available reactive sites (Kiss et al., 2022), and (2) the particle size of the GTR (>1 mm), which acts as a stress concentrator and promotes the nucleation of macro-cracks under load (Fazli and Rodrigue, 2022a). These findings agree with previous studies (Fazli and Rodrigue, 2022a; De Sousa et al., 2015), confirming that combining GTR and recycled polymers inevitably decreases the elongation at fracture properties considerably. The incorporation of rEVA (Figure 6b) modestly improved the elongation by acting as a compatibilizing bridge, thanks to its elastomeric nature (GTR-rEVA), consistent with the contact angle measurement results. However, this improvement was insufficient to reach the standards of conventional TPEs, suggesting that more effective strategies [e.g., chemical functionalization or devulcanization of GTR (Suarez Loor et al., 2024)] are required to compete with virgin materials. These results pose a clear trade-off between sustainability (use of 100% recycled materials) and mechanical performance, which should be evaluated on a case-by-case basis depending on the final application.

Finally, concerning the samples with rPA, it could be observed that the elongation at break values improved substantially for their peers without rPA, obtaining significantly improved values of 17.27% (0 wt.% rEVA), 29.26% (5 wt.% rEVA) and 30.12% (10 wt.% rEVA). These results can be supported by the decrease in the crystalline phase of the material due to the replacement of rHDPE by rPA. According to Fazli and Rodrigue (2022a), the higher the percentage of crystalline materials (rHDPE) in composite materials, the higher the stiffness and the lower the elongation at break.

3.3.2 Flexural test

Figure 7c presents the flexural modulus of the synthesized TPEs. It can be observed that both rPA and rEVA have a similar decreasing effect on the modulus. For instance, by adding only 5 wt.% of rEVA to the TPE matrix, flexural modulus experienced a 19.26% reduction (from 159.9 MPa to 129.1 MPa) and a 27.58% reduction with 5 wt.% of rPA (from 159.9 MPa to 115.8 MPa). However, the impact of having both filler and compatibilizer in the same material reduces this property drastically. For example, sample M-5rEVA-5rPA presented a modulus of 88.7 MPa, representing a 44.53% decrease. Figure 7d shows the flexural strength of TPEs, which follows a trend like flexural modulus. The addition of the compatibilizer and filler reduces flexural strength. For example, adding 10 wt.% of rEVA and 5 wt.% rPA caused a reduction of 41.50% in the unloaded sample (from 6.496 MPa to 3.8 MPa).

These modulus results can be attributed to factors such as the nature of GTR, the content of rigid thermoplastics, or the incompatibility of components. The behavior of TPEs containing GTR is influenced by particle size, degree of crosslinking, and weight percentage (Karger-Kocsis et al., 2013). Although the mentioned factors are relatively fixed, higher content of GTR leads to a softer and rubbery behavior from the overall TPE, and particle sizes smaller than 250 μm improve phase interaction (Fazli and Rodrigue, 2021). Moreover, it is crucial to consider that rHDPE content is not fixed so that flexural properties might be influenced and, thus, produce more rigid materials than similar studies (Fazli and Rodrigue, 2020b; Hazrati et al., 2018). Another factor behind rigidity could be the state of recycled EVA because reprocessing led to crosslinking, degradation (de Oliveira et al., 2018), or additive consumption. Finally, chemical and structural incompatibility will unavoidably be experienced due to the diverse nature of the phases. Consequently, voids or interfacial gaps could hinder the mechanical performance (Barbero, 2016).

In other studies, Rosana et al. (2016), TPEs have been produced for roof tile applications using ground rubber from discarded tires (NFU), recycled low-density polyethylene (rLDPE), and polyethylene terephthalate (PET). Gaggino et al. (2018), compared these recycled composite tiles with other commercial tiles under the IRAM 12528-2 standard. The recycled composite tiles exhibited excessive deformation before failure, indicating high flexibility but limited structural stiffness. In contrast, concrete tiles supported loads of up to 3,200 N with minimal deflection. Meanwhile, the TPEs analyzed in this research showed significantly lower flexural modulus values, ranging from 88.7 MPa to 159.9 MPa, and their flexural strength decreased with the addition of rEVA and rPA, reaching a minimum value of 3.8 MPa. This reduction is related to the softening effect of rEVA and the poor dispersion of the fibers, which created resin- and fiber-rich zones. Compared to structural roofing materials, TPEs lack the rigidity required for load-bearing applications, but they offer superior flexibility and resilience, making them more suitable for non-structural uses such as flooring or acoustic damping panels.

3.3.3 Izod impact resistance

The TPEs developed in this study demonstrated superior performance in energy absorption under impact (Figure 7e), significantly exceeding the threshold of 175 J/m established in the literature, without showing fracture during the tests (Kiss et al., 2022). The optimum formulation (M-10rEVA-0rPA) reached a value of 247.92 J/m, representing a substantial improvement over comparable systems previously reported (Kiss et al., 2022). These results are consistent with those obtained by Gaggino et al. (2018) under IRAM 12528-2, where their composites also did not exhibit fractures, being suitable for static applications as roof tiles in environments with severe mechanical impact (e.g., hail). The outstanding performance of these materials is attributed to the synergistic effect between GTR and rEVA. GTR, due to its elastomeric nature, inhibits crack propagation (Kiss et al., 2022), while rEVA acts as a compatibilizer, improving energy dissipation at the GTR/rHDPE interface (Li et al., 2004). On the contrary, the incorporation of rPA at five wt.% reduced the absorbed energy by 12–15% compared to formulations without fibers. This decrease is explained by the formation of agglomerates and microstructural defects, such as pores at the fiber-matrix interface, caused by the incompatibility between the polar nature of the rPA and the nonpolar matrix (Zhang et al., 2007; Fazli and Rodrigue, 2022b). The rEVA partially compensated for these effects through two mechanisms: (1) its copolymeric structure, with polar segments (acetate) interacting with the carbonyl groups of the rPA, and (2) nonpolar segments (ethylene) compatible with the rHDPE, improving interfacial adhesion. Additionally, rEVA was observed to increase the mobility of polymer chains in amorphous zones (Wang and Li, 2001), reducing stress concentrations at interfaces and improving the overall toughness of the material (Kiss et al., 2022; Rosana et al., 2016).

These findings position the developed TPEs as ideal materials for applications requiring high energy absorption and flexibility, such as outdoor roof tiles or floor slabs. Their ability to resist impacts without fracture makes them superior to conventional rigid materials.

Although the incorporation of 5 wt.% rPA resulted in a systematic deterioration of mechanical properties; their inclusion was justified by the objective of comprehensively valorizing end-of-life tire (ELT)

waste, as textile fibers constitute a significant fraction of the residual material. However, their polarity and fibrous morphology led to the formation of fiber- and resin-rich zones and agglomerations, which hindered homogeneous dispersion within the GTR/rHDPE matrix and reduced load transfer efficiency. For future research, it is proposed to enhance interfacial compatibility by reactive compatibilizing agents with polar functional groups, as demonstrated by Abraham and George (2009), who employed maleic anhydride-grafted HDPE to improve the interfacial interaction between nylon fibers and the HDPE matrix. Additionally, mechanical modifications—such as reducing fiber length before incorporation—could be considered (Zhang et al., 2007). These strategies may promote improved interfacial adhesion and mitigate agglomeration, thereby enabling the exploitation of the fibers' mechanical reinforcement potential without compromising the homogeneity of the composite.

3.3.4 Shore A hardness

Hardness is related to stiffness, and for TPEs with GTR, it has been reported to depend on the elastic modulus and degree of crosslinking of GTR (ISO7619-1, 2010). According to Figure 7f, all samples exceeded 85, and there is a slight variation among the data. Nonetheless, the addition of rPA and rEVA reduces hardness to different extents. On the one hand, hardness drops from 94.40 points to 91.46 by adding 5 wt.% of rPA; however, as fibers do not participate directly in this property, a valid origin could be the reduction of the rigid thermoplastic weight percentage (i.e., rHDPE). Finally, as rEVA is an elastomer with a certain degree of crosslinking and additives used in footwear applications, the softening effect is less significant than rHDPE. For example, at 10 wt.% of rEVA, there is a slight decrease of 1.76% compared to the base material (i.e., 70 wt.% GTR with 30 wt.% rHDPE).

3.3.5 Compression set

The formulations that exhibited positive performance were those with low compression set values, as lower values indicate a greater capacity for elastic recovery. Consequently, M-0rEVA-0rPA stood out with a value of 36.67% which belongs to a low compression set elastomer grade (Persson and Andreassen, 2022; Saleesung et al., 2010), being the only sample below the 50% limit established for TPEs (Lievana and Karger-Kocsis, 2004).

Additionally, no clear trend was identified among the results, as this property is influenced by multiple factors such as the degree of rubber crosslinking, homogeneity, crystallinity (Abraham and Barber, 2009), and the thermoplastic used (Le et al., 2020), among others. However, fibers and rEVA likely increased the heterogeneity (Sreeja, 2001) and/or allowed some degree of plastic deformation in the compound (Abraham and Barber, 2009).

3.4 Selecting the best performing material

Table 4 presents the selection matrix for the material alternatives developed by comparing the results across five categories. This matrix was constructed based on the weights assigned to each property, using a scoring system of 0, 0.5, and 1 to compare the different samples. The material alternative with the highest score was M-10rEVA-0rPA.

3.5 Proposed manufacturing process

The proposed basic manufacturing process focused on the material selection discussed in section 3.4, specifically between extrusion and cold compression molding, as illustrated in Figure 8. This selection was based on the TPE's ability to be processed in a molten state and its recyclability (Holden, 2011). The product dimensions were established according to the current market offering of rubber tiles (Activelife S.A., 2023). Finally, techno-economic and environmental analysis was carried out to assess the project's feasibility and to compare the ecological footprint with that of the conventional process (rubber tiles produced using GTR and thermoset resins) (Ecocaucho, n.d.).

3.5.1 Techno-economic analysis

Based on the analysis of financial parameters such as the Internal Rate of Return (IRR), Net Present Value (NPV), and Payback Period (RIP), several investment factors were considered, including machinery, labor, energy consumption and raw materials (Alcivar Espinoza and Risco Bravo, 2022). Additionally, the discount rate, tax rate, and inflation were considered.

Table 5 presents the estimated initial investment required for setting up the polymer processing plant.

The techno-economic analysis, based on a daily production of 800 kg of material and aligned with current tire manufacturing demand, considered the salaries of five workers, a monthly plant rental of 900 USD, and a selling price of 30 USD/m^2, determined based on an analysis of production costs and benchmarking against similar products in the market (TaurusX, n.d.). The results indicated a return time of 2 years and 5 months, an internal rate of return (IRR) of 46.87%, and a net present value (NPV) of

TABLE 4 Alternatives matrix selection.

Samples	Flexion modulus	Absorption impact energy	Shore A hardness	Specific energy consumption	Compression set	Sum	Priority
M-0rEVA-5rPA	0.003	0.000	0.060	0.010	0.053	0.127	4
M-5rEVA-5rPA	0.007	0.013	0.080	0.003	0.000	0.103	6
M-10rEVA-5rPA	0.017	0.027	0.100	0.000	0.080	0.223	2
M-0rEVA-0rPA	0.000	0.040	0.000	0.017	0.133	0.190	3
M-5rEVA-0rPA	0.010	0.053	0.020	0.013	0.027	0.123	5
M-10rEVA-0rPA	0.013	0.067	0.040	0.007	0.107	0.233	1

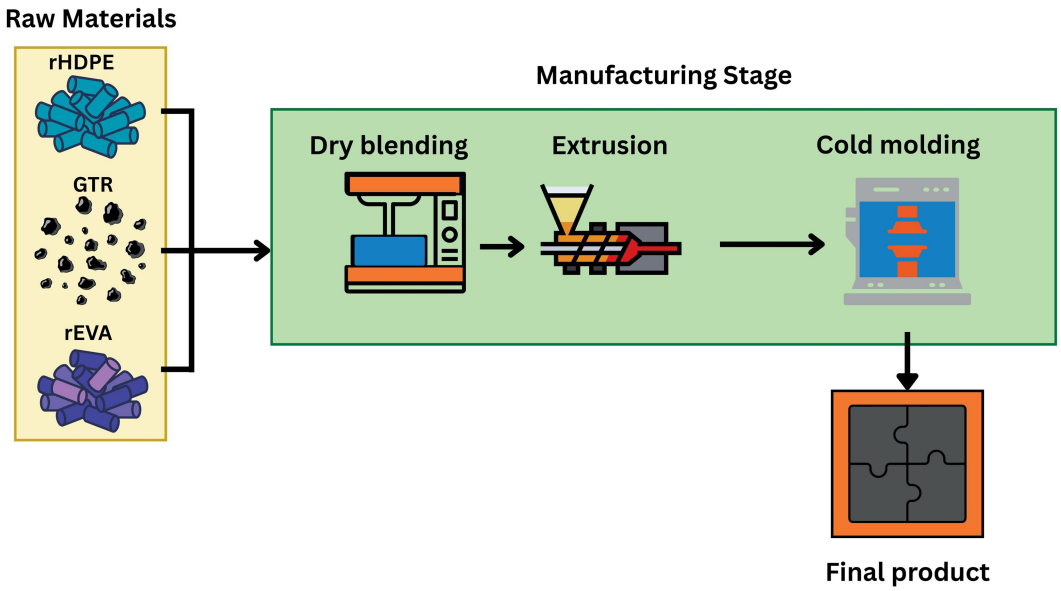

FIGURE 8
Proposed production process for rubber tiles.

117,050.61 USD. This evaluation was conducted over a 10-year projection period, with annual cost calculations applying a discount rate of 8.49%.

The Net Present Value (NPV) reflected a high and positive value, indicating the project's profitability (Stahl, 2004). Moreover, an approximate Internal Rate of Return (IRR) of 46% was obtained, which exceeds the discount rate, projecting a high potential for net earnings. Lastly, the preliminary project demonstrated a payback period of 25% of the projected lifespan, as illustrated in Figure 9, where a cash outflow was observed during the first year, associated with fixed capital expenditures and working capital requirements (Turton et al., 2018). Following this period, cash flow steadily increased, reaching a peak in year 10.

3.5.2 Eco-audit

An eco-audit was performed to quantify the energy demand and carbon footprint of producing 1 m^2 of rubber tiles. The proposed route—ambient-temperature mixing followed by short-cycle hot pressing—was benchmarked against the conventional cold mixing and prolonged hot compression process. As shown in Figure 10, the new method lowers cumulative energy demand by 32.27% and cuts the global-warming potential by 21.49% compared with the reference process. These gains arise from three main factors: (i) a shorter pressing cycle that reduces thermal energy consumption, (ii) substitution of virgin polymers with readily available recycled feedstocks, and (iii) enhanced end-of-life recyclability of the tiles (Mutlu et al., 2018).

The advantage of recycled raw materials is most pronounced in the Material phase, where their high availability and minimal preprocessing requirements translate into a 19% reduction in energy demand and a 13% decrease in carbon footprint (Ashby, 2012). In the Manufacturing phase, the conventional route exhibits a 15% lower carbon footprint because it involves fewer ancillary materials; however, its overall energy efficiency remains substantially lower than that of the proposed process. Finally, the M-10rEVA-0rPA formulation can be mechanically recycled, allowing a significant portion of its mass to be recovered as feedstock for new tiles—an option unavailable for conventional thermoset systems (Morales, 2018). This closed-loop potential confers an environmental credit in the end-of-life stage, further lowering the net impacts of the product's life-cycle assessment (Ashby, 2012).

TABLE 5 Estimation of initial fixed investment capital.

Equipment	Estimated cost (USD)
Twin Screw Extruder with a capacity of 120 kg/h (Made-in-China Connecting Buyers with Chinese Suppliers, n.d.)	35,000.00
Compression molding machine for rubber tiles with a closing pressure of 30 t (Qingdao Suiteque Machinery Co. Ltd., 2023)	13,020.00
Total	48,020.00

4 Conclusion

This study developed fully recycled thermoplastic elastomers (TPEs) from end-of-life tires (GTR and rPA fibers), recycled high-density polyethylene (rHDPE), and recycled ethylene-vinyl acetate (rEVA). The results demonstrate that rEVA acts as a compatibilizing agent by reducing the interfacial tension between GTR and rHDPE, enhancing deformability and increasing impact strength up to 247.92 J/m. However, the incorporation of rPA fibers caused agglomeration and heterogeneous zones, which led to a deterioration of the mechanical properties.

From an environmental perspective, the proposed process reduced energy consumption and carbon footprint by 32.27 and 21.49%, respectively, compared to conventional processes.

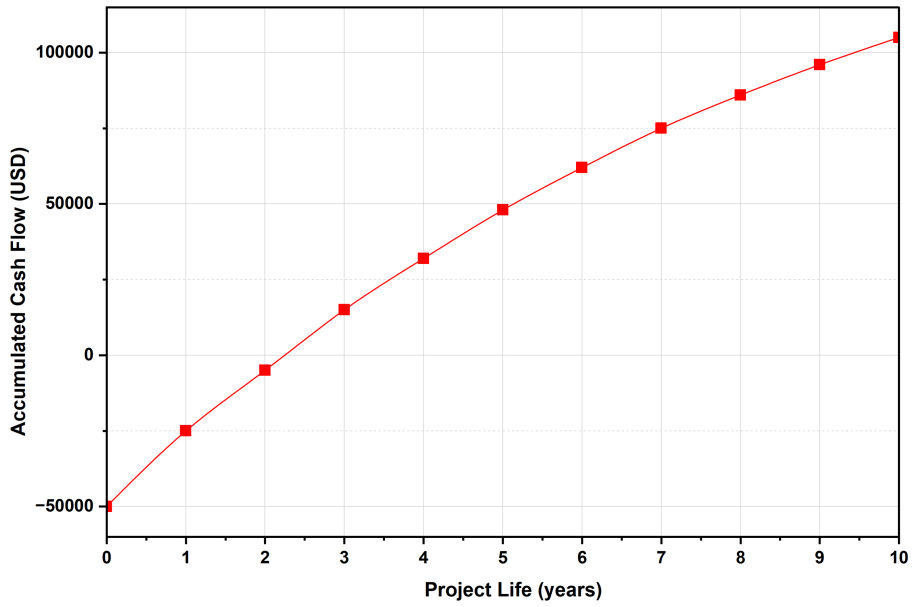

FIGURE 9
Cash flow diagram as a function of project time.

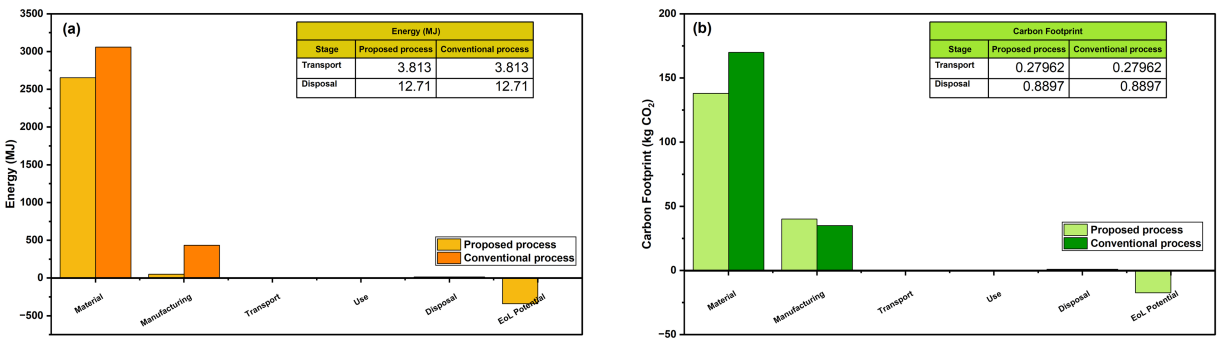

FIGURE 10
(a) Energy demand eco-audit and **(b)** Carbon footprint eco-audit.

Nevertheless, these projections rely on simplified assumptions that introduce uncertainty, particularly in cost estimation, process parameters, and energy efficiency. It is recommended that these findings be validated through more robust life-cycle assessments.

The financial analysis projected an Internal Rate of Return (IRR) of 46.87% and a payback period of 2 years and 5 months, suggesting preliminary economic feasibility. However, these results are based on idealized conditions and reference prices and should be interpreted cautiously.

Finally, it is acknowledged that the composites were not subjected to environmental aging or simulation tests, which are critical for their intended applications. Future studies should focus on accelerated aging tests and performance evaluations under real operating conditions to validate their potential use in flooring, tile products, and cushioning surfaces.

Data availability statement

The raw data supporting the conclusions of this article will be made available by the authors without undue reservation.

Author contributions

JL: Data curation, Writing – original draft, Investigation, Conceptualization. MC: Investigation, Writing – original draft, Conceptualization. ML: Investigation, Writing – review & editing, Conceptualization, Methodology. EA: Resources, Writing – review & editing. AL: Writing – review & editing, Formal analysis, Methodology. JV: Investigation, Validation, Supervision, Writing – review & editing. AC: Validation, Supervision, Writing – review & editing, Investigation.

Funding

The author(s) declare that no financial support was received for the research and/or publication of this article.

Acknowledgments

The authors thank the Laboratory of Testing Materials (LEMAT) and the Center of Nanotechnology Research and Development (CIDNA) for supporting our research during material evaluation and characterization.

Conflict of interest

The authors declare that the research was conducted in the absence of any commercial or financial relationships that could be construed as a potential conflict of interest.

Generative AI statement

The authors declare that no Gen AI was used in the creation of this manuscript.

Any alternative text (alt text) provided alongside figures in this article has been generated by Frontiers with the support of artificial intelligence and reasonable efforts have been made to ensure accuracy, including review by the authors wherever possible. If you identify any issues, please contact us.

Publisher's note

References

Abraham, T. N., and George, K. E. (2009). Short nylon fiber-reinforced HDPE: melt rheology. *J. Thermoplast. Compos. Mater.* 22, 293–304. doi: 10.1177/0892705708091612

Abraham, T., and Barber, N. (2009). Method for improving compression set in thermoplastic vulcanizates.

Acevedo, B., Fernández, A. M., and Barriocanal, C. (2015). Identification of polymers in waste Tyre reinforcing fibre by thermal analysis and pyrolysis. *J. Anal. Appl. Pyrolysis* 111, 224–232. doi: 10.1016/j.jaap.2014.11.005

Activelife S.A. (2023). Piso 2cm Interlock 50 X50. Available online at: https://activelife.ec/producto/piso-2cm-interlock-pintas-de-colores-50-x-50/?srsltid=AfmBOopiWxAuYd9i4tDChtJ_SUPl9fiShU-YWw9JwxC9cHj9AJuSuF0D (Accessed July 29, 2025).

Ahmadian, H., Yang, M., and Soghrati, S. (2020). Effect of resin-rich zones on the failure response of carbon fiber reinforced polymers. *Int. J. Solids Struct.* 188-189, 74–87. doi: 10.1016/j.ijsolstr.2019.10.004

Alcivar Espinoza, K. D., and Risco Bravo, A. N. (2022). Diseño de una propuesta sostenible de producción de biodiesel mediante optimización multiobjetivo de factores económicos, ambiental y rendimiento. Guayaquil, Ecuador: Escuela Superior Politécnica del Litoral.

Allen, N. S., Edge, M., Rodriguez, M., Liauw, C. M., and Fontan, E. Aspects of the thermal oxidation, yellowing and stabilisation of ethylene vinyl acetate copolymer. *Polymer Degrad. Stabil.* 71, 1–14. doi: 10.1016/S0141-3910(00)00111-7

Alothman, O. Y. (2012). Processing and characterization of high density polyethylene/ethylene vinyl acetate blends with different VA contents. *Adv. Mater. Sci. Eng.* 2012, 1–10. doi: 10.1155/2012/635693

Ashby, M. (2012). Materials and the environment: eco-informed material choice. *Second* Edn: Elsevier Inc., 181–184.

Badiee, A. (2016). An examination of the response of ethylene-vinyl acetate film to changes in environmental conditions. Nottingham, UK: The University of Nottingham.

Barbero, E. J. (2016). Introduction to composite materiales, vol. 15, 34.

Barcia-Quimi, A. F., Risco-Bravo, A., Alcivar-Espinoza, K., and Tinoco-Caicedo, D. L. (2023). Design of a sustainable biodiesel production process by a multi-objective optimization. *Comput. Aided Chem. Eng.* 52, 519–524. doi: 10.1016/B978-0-443-15274-0.50083-4

Biemond, G. J. E., and Gaymans, R. J. (2010). Elastic properties of thermoplastic elastomers based on poly(tetramethylene oxide) and monodisperse amide segments. *J. Mater. Sci.* 45, 158–167. doi: 10.1007/s10853-009-3911-z

Carrasco, M., Guerrero, J., Lazo, M., Adrián, E., Medina-Perilla, J. A., and Rigail-Cedeño, A. (2023). Evaluation of processing conditions in the performance of purging compounds for polypropylene injection molding. *J. Manuf. Mater. Process.* 7:7. doi: 10.3390/jmmp7010031

de Oliveira, M. C. C., Diniz Cardoso, A. S. A., Viana, M. M., and Lins, V. d. F. C. (2018). The causes and effects of degradation of encapsulant ethylene vinyl acetate copolymer (EVA) in crystalline silicon photovoltaic modules: a review. *Renew. Sust. Energ. Rev.* 81, 2299–2317. doi: 10.1016/j.rser.2017.06.039

De Sousa, F. D. B., Gouveia, J. R., De Camargo Filho, P. M. F., Vidotti, S. E., Scuracchio, C. H., Amurin, L. G., et al. (2015). Blends of ground tire rubber devulcanized by microwaves/HDPE-part B: influence of clay addition. *Polímeros* 25, 382–391. doi: 10.1590/0104-1428.1955

Ecocaucho. Primera opción de productos de caucho en Ecuador 2022. Available online at: https://www.ecocaucho.com.ec/tienda/ (Accessed July 29, 2025).

El Universo. (2024). Cuatro millones de llantas son desechadas por año en Ecuador: en cita se buscó generar buena gestión de los neumáticos. Available online at: https://www.eluniverso.com/guayaquil/comunidad/encuentro-seguridad-vial-movilidad-sostenible-seginus-utilizacion-de-neumaticos-nota/ (Accessed July 29, 2025).

Farias, G. M. G., Agrawal, P., Hanken, R. B. L., de Araújo, J. P., de Oliveira, A. D. B., and Mélo, T. J. A. (2021). Effect of EVA copolymer containing different VA content on the thermal and rheological properties of bio-based high-density polyethylene/ethylene vinyl acetate blends. *J. Therm. Anal. Calorim.* 146, 2127–2139. doi: 10.1007/s10973-020-10423-5

Fazli, A., and Rodrigue, D. (2020a). Recycling waste tires into ground tire rubber (Gtr)/rubber compounds: a review. *J. Compos. Sci.* 4, 12–20. doi: 10.3390/JCS4030103

Fazli, A., and Rodrigue, D. (2020b). Waste rubber recycling: a review on the evolution and properties of thermoplastic elastomers. *Materials* 13:782. doi: 10.3390/MA13030782

Fazli, A., and Rodrigue, D. (2021). Effect of ground tire rubber (Gtr) particle size and content on the morphological and mechanical properties of recycled high-density polyethylene (rhdpe)/gtr blends. *Recycling* 6:6. doi: 10.3390/recycling6030044

Fazli, A., and Rodrigue, D. (2022a). Thermoplastic elastomers based on recycled high-density polyethylene/ground tire rubber/ethylene vinyl acetate: effect of ground tire rubber regeneration on morphological and mechanical properties. *J. Thermoplast. Compos. Mater.* 36, 2285–2310. doi: 10.1177/08927057221095388

Fazli, A., and Rodrigue, D. (2022b). Sustainable reuse of waste Tire textile fibers (WTTF) as reinforcements. *Polymers (Basel)* 14:14. doi: 10.3390/polym14193933

Gaggino, R., Kreiker, J., Filippín, C., Sánchez Amono, M. P., González Laría, J., and Peisino, L. E. (2018). The comprehensive comparison of thermal and physical-mechanical properties of the recycled rubber and plastic roofing tiles versus roofing tiles made with different traditional materials. *Adv. Civil Eng.* 2018, 6–10. doi: 10.1155/2018/7361798

Goharpey, F., Nazockdast, H., and Katbab, A. A. (2005). Relationship between the rheology and morphology of dynamically vulcanized thermoplastic elastomers based on EPDM/PP. *Polym. Eng. Sci.* 45, 84–94. doi: 10.1002/pen.20232

Hazrati, H., Jahanbakhshi, N., and Rostamizadeh, M. (2018). Hydrophilic polypropylene microporous membrane for using in a membrane bioreactor system and optimization of preparation conditions by response surface methodology. *Polyolefins J.* 5, 97–109. doi: 10.22063/poj.2017.1945.1104

Holden, G. (2011). "Thermoplastic elastomers" in Applied plastics engineering handbook: processing and materials (Ámsterdam, Netherlands: Plastics Design Library), 77–91.

ISO7619-1 (2010). ISO 7619-1: rubber, vulcanized or thermoplastic - determination of indentation hardness - part 1: durometer method (Geneva, Switzerland: International Organization for Standardization) 2006, 13.

Kamran, M., Davidson, M. G., de Vos, S., Tsanaktsis, V., and Yeniad, B. (2022). Synthesis and characterisation of polyamides based on 2,5-furandicarboxylic acid as a

sustainable building block for engineering plastics. *Polym. Chem.* 13, 3433–3443. doi: 10.1039/d2py00189f

Karger-Kocsis, J., Mészáros, L., and Bárány, T. (2013). Ground Tyre rubber (GTR) in thermoplastics, thermosets, and rubbers. *J. Mater. Sci.* 48, 1–38. doi: 10.1007/s10853-012-6564-2

Kazemi, H., Fazli, A., Ira, J. P., and Rodrigue, D. (2023). Recycled tire fibers used as reinforcement for recycled polyethylene composites. doi: 10.20944/preprints202306.1929.v1

Kiss, L., Simon, D. Á., Petrény, R., Kocsis, D., Bárány, T., and Mészáros, L. (2022). Ground tire rubber filled low-density polyethylene: the effect of particle size. *Adv. Ind. Eng. Polym. Res.* 5, 12–17. doi: 10.1016/j.aiepr.2021.07.001

Le, H. C., Bounor-Legaré, V., Catherin, M., Lucas, A., Thèvenon, A., and Cassagnau, P. (2020). TPV: a new insight on the rubber morphology and mechanic/elastic properties. *Polymers (Basel)* 12, 1–15. doi: 10.3390/polym12102315

Li, X., Shonkwiler, S., and McMains, S. (2021). Detection of resin-rich areas for statistical analysis of fiber-reinforced polymer composites. *Compos. Part B Eng.* 225:109252. doi: 10.1016/j.compositesb.2021.109252

Li, Y., Zhang, Y., and Zhang, Y. (2004). Morphology and mechanical properties of HDPE/SRP/elastomer composites: effect of elastomer polarity. *Polym. Test.* 23, 83–90. doi: 10.1016/S0142-9418(03)00065-5

Lievana, E., and Karger-Kocsis, J. (2004). Use of ground Tyre rubber (GTR) in thermoplastic polyolefin elastomer compositions. *Prog. Rubber. Plast. Recycl. Technol.* 20, 1–10. doi: 10.1177/147776060402000101

Liu, S., Peng, Z., Zhang, Y., Rodrigue, D., and Wang, S. (2022). Compatibilized thermoplastic elastomers based on highly filled polyethylene with ground tire rubber. *J. Appl. Polym. Sci.* 139, 6–8. doi: 10.1002/app.52999

Made-in-China Connecting Buyers with Chinese Suppliers. Plastic compounding twin screw extruder with competitive price 2023. Available online at: https://www.made-in-china.com/manufacturers/plastic-compounding-twin-screw-extruder.html (Accessed July 29, 2025).

Mészáros, L., Tábi, T., Kovács, J. G., and Bárány, T. (2008). The effect of EVA content on the processing parameters and the mechanical properties of LDPE/ground tire rubber blends. *Polym. Eng. Sci.* 48, 868–874. doi: 10.1002/pen.21022

Ministerio del Ambiente A y TE. Ecuador presentó la hoja de ruta para reducir impactos por la contaminación de plásticos 2022. Available online at: https://www.ambiente.gob.ec/ecuador-presento-la-hoja-de-ruta-para-reducir-impactos-por-la-contaminacion-de-plasticos/ (Accessed July 29, 2025).

Morales, I. R. (2018). "Recycling of thermosets and their composites" in Thermosets: structure, properties, and applications. *2nd* ed (Elsevier), 639–666.

Mutlu, V., Özgür, C., and Kaplan Bekaroğlu, Ş. Ş. (2018). Determination of carbon footprint in rubber industry. *Bilge Int. J. Sci. Technol.* 2, 139–146. doi: 10.30516/bilgesci.434223

Naat, J. N., Neolaka, Y. A. B., Lapailaka, T., Rachmat Triandi, T., Sabarudin, A., Darmokoesoemo, H., et al. (2021). Adsorption of Cu(II) and Pb(II) using silica@mercapto (hs@m) hybrid adsorbent synthesized from silica of Takari sand: optimization of parameters and kinetics. *Rasayan J. Chem.* 14, 550–560. doi: 10.31788/RJC.2021.1415803

Palakattukunnel, S. T., Thomas, S., Sreekumar, P. A., and Bandyopadhyay, S. (2011). Poly(ethylene-co-vinyl acetate)/calcium phosphate nanocomposites: contact angle, diffusion and gas permeability studies. *J. Polym. Res.* 18, 1277–1285. doi: 10.1007/s10965-010-9530-1

Panwar, K., Jassal, M., and Agrawal, A. K. (2015). In situ synthesis of Ag-SiO_2 janus particles with epoxy functionality for textile applications. *Particuology* 19, 107–112. doi: 10.1016/j.partic.2014.06.007

Patrício, J., Andersson-Sköld, Y., and Gustafsson, M. (2021). End-of-life tyres applications: technologies and environmental impacts (VTI rapport 1100A).

Periasamy, K., Kandare, E., Das, R., Darouie, M., and Khatibi, A. A. (2023). Interfacial engineering methods in thermoplastic composites: an overview. *Polymers (Basel)* 15:15. doi: 10.3390/polym15020415

Persson, A. M. M. R., and Andreassen, E. (2022). Cyclic compression testing of three elastomer types— a thermoplastic vulcanizate elastomer, a liquid silicone rubber and two ethylene-propylene-diene rubbers. *Polymers (Basel)* 14, 1–2. doi: 10.3390/polym14071316

Qingdao Suiteque Machinery Co. Ltd. (2023). Rubber Paver Tile Vulcanizing Press/Interlock Rubber Tiles Hydraulic Press/Rubber Floor Hot Molding Press. Available online at: https://oulimachine.en.made-in-china.com/product/DdWtfvBcLSrX/China-Rubber-Paver-Tile-Vulcanizing-Press-Interlock-Rubber-Tiles-Hydraulic-Press-Rubber-Floor-Hot-Molding-Press.html (Accessed July 29, 2025).

Ramarad, S., Khalid, M., Ratnam, C. T., Chuah, A. L., and Rashmi, W. (2015). Waste tire rubber in polymer blends: a review on the evolution, properties and future. *Prog. Mater. Sci.* 72, 100–140. doi: 10.1016/j.pmatsci.2015.02.004

Rigail-Cedeño, A., Lazo, M., Gaona, J., Delgado, J., Tapia-Bastidas, C. V., Rivas, A. L., et al. (2022). Processability and physical properties of compatibilized recycled HDPE/rice husk biocomposites. *J. Manuf. Mater. Process.* 6:67. doi: 10.3390/jmmp6040067

Rosana, G., Maria, P., Jerónimo, K., Paz, S. A. M., Ricardo, A., and Carlos, B. J. (2016). Cover system for roofs manufactured with recycled polyethylene and rubber. *Key Eng. Mater.* 668, 348–356. doi: 10.4028/www.scientific.net/KEM.668.348

Saleesung, T., Saeoui, P., and Sirisinha, C. (2010). Mechanical and thermal properties of thermoplastic elastomer based on low density polyethylene and ultra-fine fully-vulcanized acrylonitrile butadiene rubber powder (UFNBRP). *Polym. Test.* 29, 977–983. doi: 10.1016/j.polymertesting.2010.08.008

Sebaey, T. A., Bouhrara, M., and O'dowd, N. (2021). Fibre alignment and void assessment in thermoplastic carbon fibre reinforced polymers manufactured by automated tape placement. *Polymers (Basel)* 13:1–12. doi: 10.3390/polym13030473

Seginus. Sustainability report 2025. https://seginus.com.ec/en/home-en/ (Accessed July 29, 2025).

Sreeja, T. D. (2001). Studies on short nylon fiber-reclaimed rubber/elastomer composites.

Stahl, M. (2004). "Net Present Value (NPV)" in Encyclopedia of health care management, 1–3.

Suarez Loor, J., Lazo, M., Rigail, A., Adrian, E., and Vera, J. (2024). Processing of thermoplastic elastomers (TPE) by in-situ ground tire rubber (GTR) vulcanization using waste ethylene-vinyl-acetate (wEVA) and dicumyl peroxide (DCP). Bogotá, Colombia: Ediciones Uniandes.

TaurusX (n.d.). Supermercado del Fitness. Available online at: https://taurusecuador.com/product-category/pisos/ (Accessed July 29, 2025).

Tham, D. Q., Trang, N. T. T., Chinh, N. T., Giang, N. V., Lam, T. D., and Hoang, T. (2016). Sustainable composite materials based on ethylene-vinylacetate copolymer and organo-modified silica. *Green Process. Synth.* 5, 557–566. doi: 10.1515/gps-2016-0044

Turton, R., Shaeiwitz, J., Bhattacharyya, D., and Whiting, W. (2018). Analysis synthesis and design of chemical processes. *5th* Edn. Upper Saddle River, New Jersey, EE. UU.: Pearson Education, Inc.

van Hoek, J. W., Heideman, G., Noordermeer, J. W. M., Dierkes, W. K., and Blume, A. (2019). Implications of the use of silica as active filler in passenger car tire compounds on their recycling options. *Materials* 12, 1–19. doi: 10.3390/ma12050725

Wade, L., and Simek, J. (2012). Organic chemistry. *7th* Edn. Mexico City: Pearson Education.

Wang, H., Apostolidis, P., Zhu, J., Liu, X., Skarpas, A., and Erkens, S. (2021). The role of thermodynamics and kinetics in rubber–bitumen systems: a theoretical overview. *Int. J. Pavement Eng.* 22, 1785–1800. doi: 10.1080/10298436.2020.1724289

Wang, X., and Li, H. (2001). Compatibilizing effect of ethylene-vinyl acetate-acrylic acid copolymer on nylon 6/ethylene-vinyl acetate copolymer blended system: mechanical properties, morphology and rheology. *J. Mater. Sci.* 36, 5465–5473. doi: 10.1023/A:1012437832479

Yilmaz, Z. (2007). Enhancement of compatibility of polyethylene/polyvinyl acetate blends by irradiation of polyethylene. Ankara, Turkey: Hacettepe Üniversitesi Akademik Veri Yönetim Sistemi.

Zhang, X. X., Lu, C. H., and Liang, M. (2007). Preparation of rubber composites from ground tire rubber reinforced with waste-tire fiber through mechanical milling. *J. Appl. Polym. Sci.* 103, 4087–4094. doi: 10.1002/app.25510